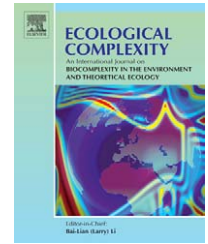


available at www.sciencedirect.comjournal homepage: <http://www.elsevier.com/locate/ecocom>

Complex spatiotemporal dynamics in Lotka–Volterra ring systems

J.C. Wildenberg, J.A. Vano, J.C. Sprott *

Department of Physics, University of Wisconsin, Madison, Wisconsin 53706, USA

ARTICLE INFO

Article history:

Received 10 October 2005

Received in revised form

5 December 2005

Accepted 10 December 2005

Keywords:

Lotka–Volterra

Competition

Ecology

Chaos

Lyapunov function

ABSTRACT

Mathematical models in ecology often need to incorporate spatial dependence to accurately model real-world systems. We consider competitive Lotka–Volterra models modified to include this spatial dependence through organization of the competing species into a one-dimensional ring by an appropriate choice of the interaction matrix. We show that these systems can exhibit complex dynamics, spatiotemporal chaos, and spontaneous symmetry breaking. A high-dimensional, spatially homogeneous, nearest-neighbor example with interaction strengths decreasing with distance is characterized including an analysis of how the dynamics of the system vary with dimension. We also show the existence of Lyapunov functions that arise from this method of including spatial dependence and how they prohibit complex dynamics for certain regions of the parameter space. We utilize these Lyapunov functions to reduce the required calculation time in brute-force searches of parameter space. A short comparison is given to derived line systems including a contrast between the eigenvalues of the two systems.

© 2006 Published by Elsevier B.V.

1. Introduction

Mathematical models are often used in ecology to describe the behavior of real-world systems (May, 1973; Freedman, 1987; Takeuchi, 1996). A very general model, derived independently by Lotka (1925) and Volterra (1926), allows different species to interact through non-linear coupling

$$\frac{dx_i}{dt} = g_i x_i \left(1 - \sum_{j=1}^N a_{ij} x_j \right) \quad (1)$$

In this form g_i represents the linear growth rate of species i and $A = (a_{ij})$ is the interaction matrix with a_{ij} representing the interaction of species i with species j (the interaction between species is not necessarily symmetric, and in general $a_{ij} \neq a_{ji}$). Without loss of generality one can set all $g_i = a_{ii} = 1$. This is

equivalent to measuring each population x_i in terms of the carrying capacity in the absence of other species, and the time in units of inverse growth rate for each species (Coste et al., 1979). The purely competitive version of this model requires that all $a_{ij} \geq 0$ and has the benefit of constraining all populations x_i to the interval $(0,1)$, effectively bounding the solution (Murray, 1989).

When considering real-world systems one may need to incorporate some spatial dependence into the mathematical model. Some work has been done in which the spatial system is a Markov process on a lattice (Provada and Tsekouras, 2003) or the system includes a stochastic variable (Neuhauser and Pacala, 1999). High dimensional simulations on a 2-D lattice using predator–prey systems have also been carried out; however, these systems allow the type of species at each lattice point to vary (Wilson et al., 1993). We use an explicitly

* Corresponding author. Tel.: +1 608 263 4449; fax: +1 608 262 7205.

E-mail addresses: jcwildenberg@wisc.edu (J.C. Wildenberg), jvano@math.wisc.edu (J.A. Vano), sprott@physics.wisc.edu (J.C. Sprott).
1476-945X/\$ – see front matter © 2006 Published by Elsevier B.V.
doi:10.1016/j.ecocom.2005.12.001

$$A = \begin{bmatrix} 1 & a_1 & 0 & 0 & 0 & a_{-1} \\ a_{-1} & 1 & a_1 & 0 & 0 & 0 \\ 0 & a_{-1} & 1 & a_1 & 0 & 0 \\ 0 & 0 & a_{-1} & 1 & a_1 & 0 \\ 0 & 0 & 0 & a_{-1} & 1 & a_1 \\ a_1 & 0 & 0 & 0 & a_{-1} & 1 \end{bmatrix}$$

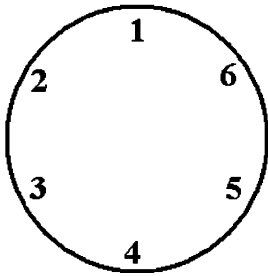


Fig. 1 – An example of how the interaction matrix can be chosen to produce a spatially-dependent Lotka-Volterra system. This ring has each (identical) species interacting only with its neighbor species on each side. This six-species ring will not admit periodicity or chaos due to the presence of a Lyapunov function (see Section 4). However, periodicity and chaos are possible through the addition of more interaction terms.

deterministic model with modifications to the interaction matrix instead of changes to the structure of the Lotka-Volterra equations. A straightforward way to add this spatial dependence is to choose the interaction matrix such that the species are aligned in some spatial arrangement and therefore interact only with their near neighbors. For example, it is possible to align the species in a one-dimensional ring through specific organization of the matrix A . The following example creates a ring with N identical species (we only consider systems of identical species, but this organization of the interaction matrix can be used for any number of non-identical species). Begin by choosing interaction coefficients for the first species (row 1 of A) assuming that species two is immediately to the right of species one, species N immediately to the left of species one, etc. All species are identical, and to generate row i of A simply shift the first row by $(i - 1)$ as shown in Fig. 1 (i runs from 1 to N and is assumed to wrap, e.g. $x_{N+1} = x_1$, to create periodic boundary conditions). This organization of the interaction matrix provides a method for incorporating spatial dependence without using more complex reaction-diffusion strategies, which modify the fundamental Lotka-Volterra equations (Cantrell and Cosner, 2003). However, the resulting models are not realistic if they do not exhibit complex dynamics. Many parameter values result in the populations attracting to an equilibrium point and are therefore not representative of real-world systems, few of which are static. Some low-dimensional ring systems have been studied which admit periodic orbits, but these systems do not contain the quadratic self-interaction term

common to many Lotka-Volterra equations (Frachbourg et al., 1996).

A simple Lotka-Volterra ring system that exhibits explicit spatial dependence and complex dynamics is

$$\frac{dx_i}{dt} = x_i(1 - a_{-2}x_{i-2} - a_{-1}x_{i-1} - x_i - a_1x_{i+1} - a_2x_{i+2}) \quad (2)$$

in which each species competes only with the two neighbors on each side.

In real-world systems, species will rarely be capable of recovery if their population drops too low. Here, we use a threshold of 10^{-6} as the point at which a species is assumed to become extinct (Ovaskainen and Hanski, 2003). A search to maximize the largest Lyapunov exponent for $N = 100$, while maintaining populations above the aforementioned threshold to prevent extinction, resulted in a system with interaction values

$$a_{-2} = 0.451, a_{-1} = 0.505, a_1 = 0.852, a_2 = 0.237 \quad (3)$$

which are henceforth assumed for Eq. (2) unless otherwise specified. The system is weakly chaotic with a largest Lyapunov exponent $\lambda_1 \cong 0.00394$. The five largest Lyapunov exponents are all positive, and the Kaplan-Yorke dimension $D_{KY} \cong 11.28$ (Kaplan and Yorke, 1979). There are 2^N equilibria including the coexisting equilibrium point given by

$$p_i = \frac{1}{\sum_{j=1}^N a_{ij}} = \frac{1}{a_{-2} + a_{-1} + 1 + a_1 + a_2} \quad (4)$$

for interaction matrices created with the above method (more about these matrices in Section 4). Under conditions (3) $p_i = 0.328407\dots$ for all i due to the homogenous nature of this system. The interaction strength decreases with distance, mirroring what one expects in most real-world spatial systems. The eigenvalues of the Jacobian expanded about the coexisting equilibrium point indicate that there are 10

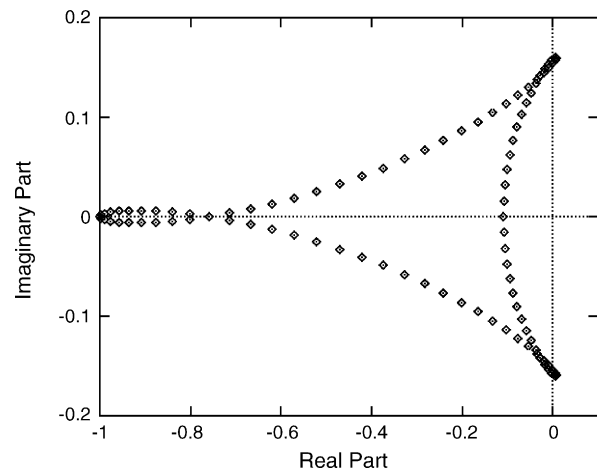


Fig. 2 – The eigenvalues for Eq. (2) with condition (3) and $N = 100$ exhibit a distorted trefoil shape. There are 10 eigenvalues with positive real parts (unstable directions) and 90 with negative real parts (stable directions). This implies that the equilibrium point at $p_i = 0.328407\dots$ for all i is an index-10 spiral saddle.

104 unstable directions and 90 stable directions (Fig. 2). The equi-
105 librium is thus an index-10 spiral saddle (Sprott, 2003).

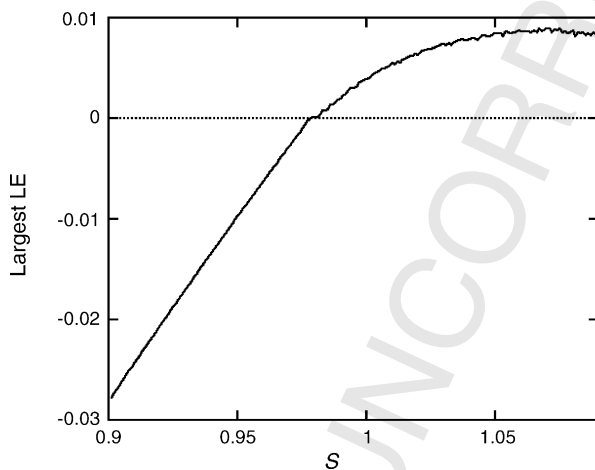
106 A simpler choice of parameters results in the model

$$107 \frac{dx_i}{dt} = x_i(1 - ax_{i-2} - x_i - bx_{i+1}) \quad (5)$$

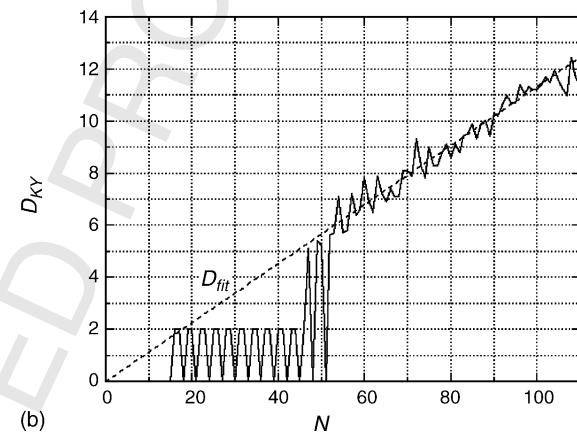
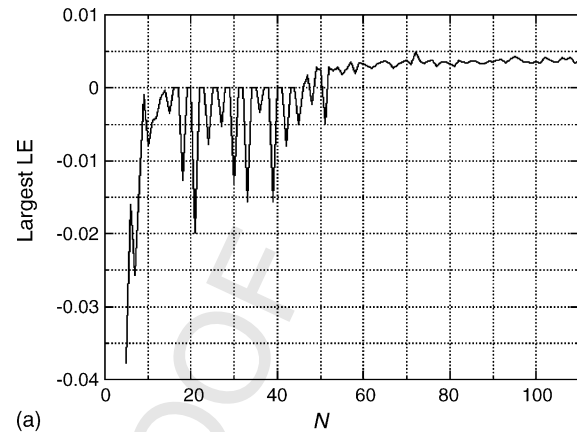
108 which is described in-depth by Sprott et al. (in press). This
109 system is very mathematically elegant, chaotic with $a = b = 1$
110 for $N > 65$, and works well to illustrate general properties of
111 Lotka–Volterra ring systems, but it is not a very realistic real-
112 world model due to its improbable connectivity. An extensive
113 search of homogeneous ring models with only one interaction
114 term (other than the self-interaction) has not found chaos or
115 periodicity for any parameter values.
116
117

118 2. Routes to chaos

119 If we define a parameter s that multiplies all of the off-diagonal
120 elements in the interaction matrix of Eq. (2) we have a variable
121 to control the strength of the interactions around the ring ($s = 1$
122 unless otherwise stated). At $s = 0$ the ring is completely
123 decoupled and the systems acts as N independent Verhulst
124 (logistic) equations, while at $s = \infty$ there is maximal competi-
125 tion and only one species can survive. A scan over s reveals
126 that this system has a very small periodic/quasi-periodic
127 region with one or more of its largest Lyapunov exponents
128 equal to zero, and a large chaotic region (Fig. 3). The Hopf
129 bifurcation, where the equilibrium point first becomes
130 unstable due to a complex conjugate pair of eigenvalues
131 having real parts exactly equal to zero, occurs at $s \approx 0.9781$ for
132 $N = 100$ and varies with N as the eigenvalues rotate about the
133 trefoil shape (Wildenberg et al., 2005). Varying the dimension



134 **Fig. 3 – The largest Lyapunov exponent plotted over the**
135 **bifurcation parameter s for Eq. (2) ($N = 100$) shows almost**
136 **no periodic region (largest Lyapunov exponent equal to**
137 **zero). Above the Hopf bifurcation at $s \approx 0.979$ the system**
138 **quickly becomes chaotic at $s \approx 0.985$. At high values of s**
139 **(not shown) the extreme competition between species**
140 **causes some to go extinct. At the limit of high s only one**
141 **species will survive and the rest will die due to the**
142 **increased competition.**



134 **Fig. 4 – The dimensionality of the system N provides a**
135 **discrete bifurcation parameter: (a) the largest Lyapunov**
136 **exponent oscillates between negative values and zero at**
137 **low N and remains positive for $N \geq 52$; and (b) the**
138 **dimension of the attractor follows the largest Lyapunov**
139 **exponent, oscillating between an equilibrium point and a**
140 **two-torus for small N , and is not an integer when the**
141 **system is chaotic, indicating a strange attractor. A**
142 **regression line fitted to the chaotic cases follows the**
143 **equation $D_{\text{fit}} = 0.11N - 0.01$.**

134 N of the system provides a discrete route to chaos. The largest
135 Lyapunov exponent and dimensionality of the attractor (non-
136 integer values represent fractal structure) fluctuate at lower
137 dimensions (Fig. 4). For all $N \geq 52$ the system is chaotic, and the
138 dimension seems to increase linearly with N according to the
139 equation

$$140 D_{\text{fit}} = 0.11N - 0.01 \quad (6)$$

141 The dimension is slow to converge, and it is possible that a
142 longer calculation would have the intercept of Eq. (6) approach
143 zero.
144
145

146 3. Spatiotemporal patterns

147 Positive initial conditions with all x_i identical for Eq. (2) with
148 conditions (3) attract to the coexisting equilibrium point.
149 These initial conditions lie on the 90-dimensional stable

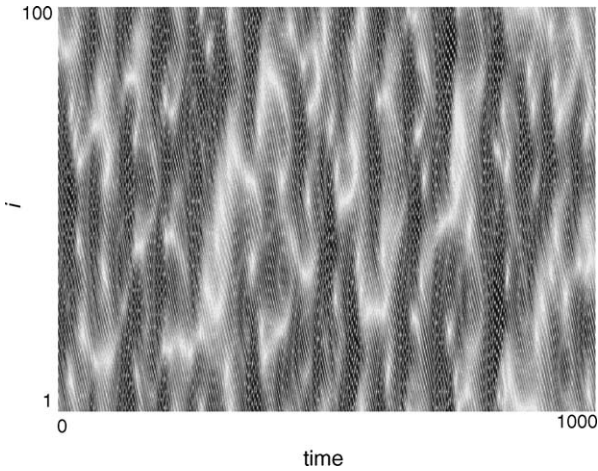


Fig. 5 – The magnitude of the spatial derivative $|x_i - x_{i-1}|$ about the ring over time for Eq. (2) with $N = 100$. The spatiotemporal chaos ensures that the patterns seen in the plot will never repeat. Although the equations describing the system are homogenous, the solution is heterogeneous and is an example of spontaneous symmetry breaking.

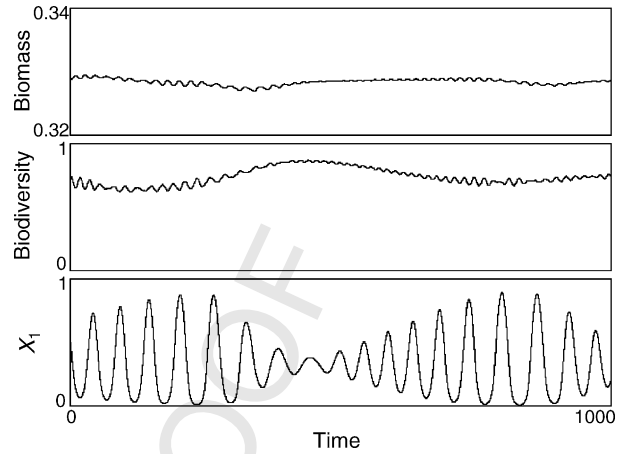


Fig. 7 – Plots of the biomass, biodiversity, and a typical $x(t)$ for Eq. (2) and $N = 100$ exhibit chaotic fluctuations. The primary oscillation of x_1 occurs at a frequency $\omega \cong 0.13$. The biomass seems to exhibit a power spectrum that exponentially decreases with increasing frequency while the biodiversity has a more broadband power spectrum with a dominant component at $\omega \cong 0.38$. This results in the biodiversity oscillating approximately three times for every oscillation of x_1 .

manifold, which constitutes a set of measure zero in the 100-dimensional state space. Most non-identical positive initial conditions approach the strange attractor. The connectivity of the ring allows fluctuations of the species populations to propagate and gives rise to spatiotemporal patterns (Fig. 5). Here, the magnitude of the spatial derivative, $|x_i - x_{i-1}|$, is plotted over space and time and serves to show the patterns while suppressing the oscillations that result from the tendency for neighboring species to fluctuate out of phase. Such a plot illustrates spontaneous symmetry breaking and results in a heterogeneous solution to a system with

homogenous equations (Turing, 1952; Meinhardt, 1982; Brading and Castellani, 2003). One can also view the spatiotemporal structure using the cross-correlation formula

$$C(\Delta i, \Delta t) = \frac{|\int [x_{N/2}(t) - x][x_{N/2+\Delta i}(t + \Delta t) - x] dt|}{\int [x_{N/2}(t) - x]^2} \quad (7)$$

with

$$x = \lim_{T \rightarrow \infty} \frac{1}{T} \int_0^T x_{N/2}(t) dt \quad (8)$$

the mean value of x_i (Spratt et al., in press). Fig. 6 shows, for $N = 100$, the dispersion at $\Delta t = 0, 50$, and 100 . Only the even values of i are plotted to suppress the fluctuations mentioned above. Note that the dispersion is not symmetric in space due to the asymmetry in the rows of the interaction matrix.

Another way to view the chaotic dynamics is through plots of the biomass

$$M = \frac{1}{N} \sum_{i=1}^N x_i \quad (9)$$

and the biodiversity (Spratt, 2004)

$$D = 1 - \frac{1}{2(N-1)} \sum_{i=1}^N \left| \frac{x_i}{M} - 1 \right| \quad (10)$$

as shown in Fig. 7. The most dominant frequency of the three signals is the oscillation in x_1 with $\omega \cong 0.13$. This value is close to the linear frequency of the most unstable complex conjugate pair of eigenvalues for which $\omega \cong 0.1592$. The biomass seems to exhibit a power spectrum that exponentially decreases with increasing frequency while the biodiversity

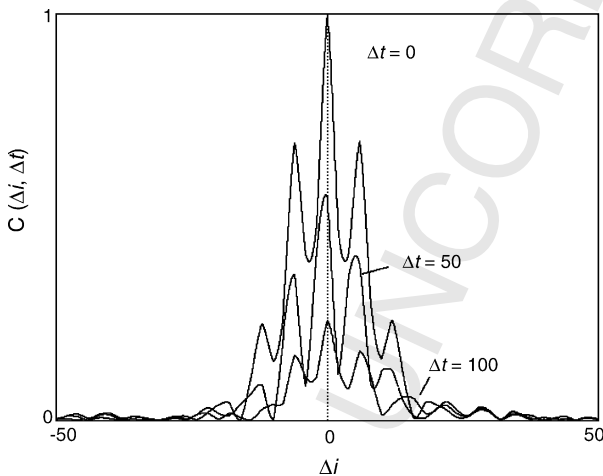


Fig. 6 – The spatiotemporal cross-correlation function plotted over time shows the propagation and dispersion common to Lotka-Volterra ring systems. The plot is not symmetric due to the asymmetry in the rows of the interaction matrix, though there does seem to be a spatial periodicity of $\Delta i = 6$ in both directions.

188 has a more broadband power spectrum with a dominant
 189 component at $\omega \cong 0.38$; oscillating approximately three times
 190 for every oscillation in x_1 .

191 **4. Lyapunov functions**

192 Suppose

193
$$X = \begin{pmatrix} x_1 \\ x_2 \\ \vdots \\ x_N \end{pmatrix} \quad (11)$$

194 is an autonomous system given by $\dot{X} = f(X)$ with an equi-
 195 librium point p such that $f(p) = 0$. If there exists a continuous
 196 scalar function $L(X)$ with continuous first partial derivatives in
 197 a region D containing p with $L(p) = 0$ and $L(X) > 0$ for all other X
 198 in D , and furthermore if the time derivative of $L(X)$ with respect
 199 to the system X

200
$$\dot{L}(X) = \nabla L(X)\dot{X} \quad (12)$$

201 is negative semi-definite ($\dot{L}(p) = 0$ and $\dot{L}(X) \leq 0$ for all other X
 202 in D) then $L(X)$ is a Lyapunov function and the equilibrium
 203 point is stable. If $\dot{L}(X) < 0$ (negative definite) then the equi-
 204 librium point is asymptotically stable (LaSalle and Lefschetz,
 205 1961; Boyce et al., 1986). A negative definite derivative implies
 206 that $L(X)$ decreases along all orbits and in many systems may
 207 behave as an energy function. The existence of a Lyapunov
 208 function with asymptotic stability prevents periodic, quasi-
 209 periodic, and chaotic behavior in the system since all orbits
 210 must attract to the equilibrium point (Xue-Zhi et al., 1999;
 211 Pykh, 2001). Although it is difficult to determine the explicit
 212 form of a Lyapunov function (even if its existence can be
 213 shown), there have been some attempts to create algorithms
 214 for Lyapunov function construction (Poincaré, 1881; Oguztoreli
 215 et al., 1981).

216 Creation of a spatially-dependent competitive Lotka-
 217 Volterra system with identical species via shifts of the rows
 218 in the interaction matrix results in a circulant matrix (Davis,
 219 1994). If we let C be the circulant matrix

220
$$C = \begin{bmatrix} c_0 & c_1 & \dots & c_{N-1} \\ c_{N-1} & c_0 & \dots & c_{N-2} \\ \vdots & \vdots & \ddots & \vdots \\ c_1 & c_2 & \dots & c_0 \end{bmatrix} \quad (13)$$

221 and γ be the N th root of unity, $\gamma = e^{i2\pi/N}$, then the eigenvalues
 222 of C are (Hofbauer and Sigmund, 1988)

223
$$\lambda_k = \sum_{j=0}^{N-1} c_j \gamma^{kj} \text{ for } k = 0, \dots, N-1 \quad (14)$$

224 If $\text{Re}(\lambda_k) > 0$ for $k \in \mathbf{Z}$, $0 < k \leq N/2$ then a Lyapunov function
 225 exists, and the orbit of this system must attract to the coex-
 226 isting equilibrium point (Zeeman, 1997; van den Driessche and
 227 Zeeman, 1998).

228 All interaction matrices created by the method described in
 229 Section 1 are circulant, and thus for Eq. (5)

230
$$\lambda_k = 1 + ae^{i2\pi(N-2)k/N} + be^{i2\pi k/N} \quad (15)$$

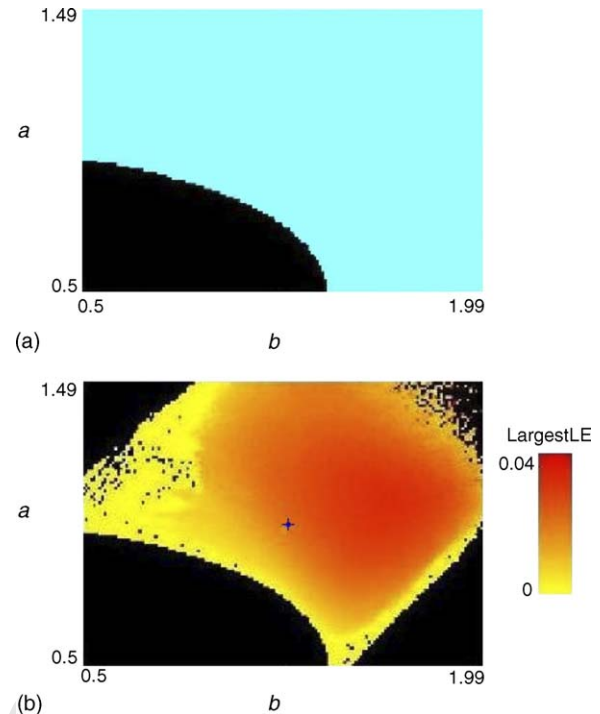


Fig. 8 – (a) The regions of parameter space for Eq. (5) (with $N = 100$) where a Lyapunov function exists and therefore the orbit must approach an equilibrium point (black) and the regions where more complex dynamics are allowed (light blue); and (b) the largest Lyapunov exponent over the same region of parameter space. The black regions represent parameter values where the orbit attracts to an equilibrium point (largest Lyapunov exponent less than zero). Notice how the region where complex dynamics is forbidden by the existence of a Lyapunov function in (a) closely matches the region where the orbit attracts to an equilibrium point in the lower left of (b). The blue cross in (b) shows $a = b = 1$.

231 The system will not be periodic, quasi-periodic, or chaotic
 232 if

233
$$\text{Re}(\lambda_k) = 1 + a \cos\left(\frac{4\pi k}{N}\right) + b \cos\left(\frac{2\pi k}{N}\right) > 0 \quad (16)$$

234 for all $1 \leq k \leq N/2$. A plot of the regions where the Lyapunov
 235 function exists in parameter space next to a plot over a and b of
 236 the largest Lyapunov exponent clearly shows that a large
 237 region where the orbit attracts to an equilibrium point can
 238 be explained by this Lyapunov function (Fig. 8).

239 The extra terms in Eq. (2) complicate the eigenvalues
 240 slightly but, utilizing some algebra,

241
$$\lambda_k = 1 + a_{-2}e^{i2\pi(N-2)k/N} + a_{-1}e^{i2\pi(N-1)k/N} + a_1e^{i2\pi k/N} + a_2e^{i4\pi k/N} \quad (17)$$

242 which implies that if

243
$$\text{Re}(\lambda_k) = 1 + (a_{-2} + a_2)\cos\left(\frac{4\pi k}{N}\right) + (a_{-1} + a_1)\cos\left(\frac{2\pi k}{N}\right) > 0 \quad (18)$$

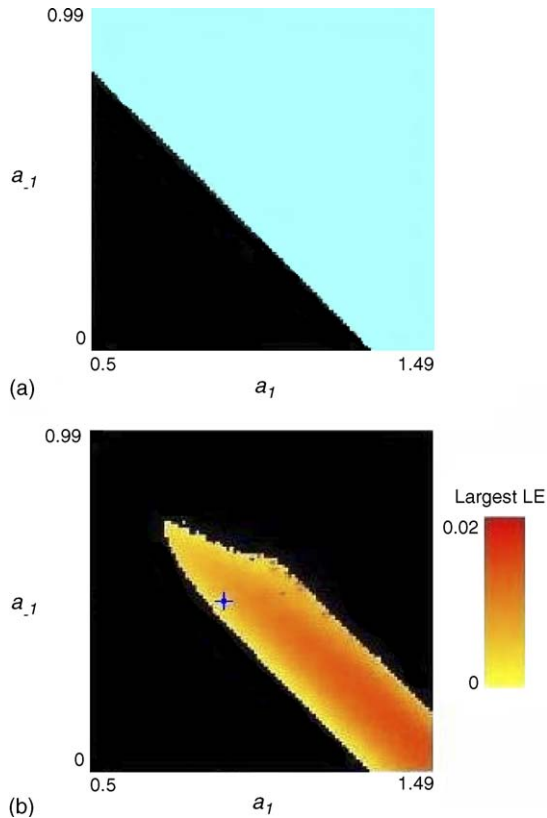


Fig. 9 – (a) The region of parameter space for Eq. (2) where the Lyapunov function exists is shown in black (and the orbit must attract to an equilibrium point) and the region where complex dynamics is possible in light blue; and (b) black areas are where the orbit attracts to the equilibrium point. The black region in (a) closely matches the black region in the lower left of (b). In these scans $a_{-2} = 0.451$ and $a_2 = 0.237$. The blue cross in (b) indicates condition (3), considered throughout the paper.

for all $1 \leq k \leq N/2$ then the orbit must attract to the coexisting equilibrium point. Fig. 9 shows that, as with Eq. (5), a scan over a_{-1} and a_1 with $a_{-2} = 0.451$ and $a_2 = 0.237$ for $N = 100$ reveals a large region of parameter space where the orbit attracts to the equilibrium point attributable to the existence of the Lyapunov function.

As a result, since all spatially homogeneous Lotka–Volterra systems have a circulant interaction matrix, a Lyapunov function will exist for certain regions of the parameter space, and any complex dynamics must occur outside those regions. Note that the disappearance of this Lyapunov function is equivalent to the Hopf bifurcation; however, the occurrence of a Hopf bifurcation does not in general imply that a Lyapunov function existed prior to the bifurcation. Similar analysis shows that any spatial system with symmetric interactions ($a_{i-1} = a_{i+1}$, $a_{i-2} = a_{i+2}$, etc.) has a Lyapunov function regardless of the specific interaction values and thus cannot exhibit complex dynamics (the actual requirement is completely symmetric interactions such that $a_{ij} = a_{ji}$ for all $i \neq j$, but spatial systems with symmetric interactions are a subset (MacArthur, 1970; Pykh, 2001)). Another Lyapunov function prevents only

near-neighbor systems, such as the one in Fig. 1, from exhibiting complex dynamics (Pykh, 2001). Lyapunov functions are difficult to find, and other regions in Figs. 8 and 9 where the orbit attracts to an equilibrium point may be due to the presence of different Lyapunov functions. Calculation of the largest Lyapunov exponent for high-dimensional systems requires significant computational resources, while a calculation of where a (known) Lyapunov function exists is trivial. Therefore, knowledge of the explicit form of possible Lyapunov functions may be used to expedite numerical brute-force searches in parameter space.

5. Line systems

Complex dynamics also seem possible if the boundary conditions are not periodic. A line can be created from a ring through many methods including severing the ring through removal of the interaction terms in the upper right and lower left corners of the interaction matrix A , holding the populations of the end species fixed, or reflecting the severed connections onto the species of the opposite side. Although these systems are not constrained by the Lyapunov function described above, there are most likely different Lyapunov functions, and a numerical scan of the parameter space reveals it to be more restricted than the ring systems, resulting in a narrower range where complex dynamics occur. This can be seen visually by comparing the eigenvalues of Eq. (5) and those of a derived line system formed by reflection of the interactions at the boundary. For the line system the Hopf bifurcation will occur at a larger value of the bifurcation parameter s , which effects the size of the eigenvalue structure, as the most positive real part is less than that of the ring system (Fig. 10). The figure also shows that as N gets large the eigenvalues of the line approach those of the ring. This may be due to the concept that an infinitely long line is

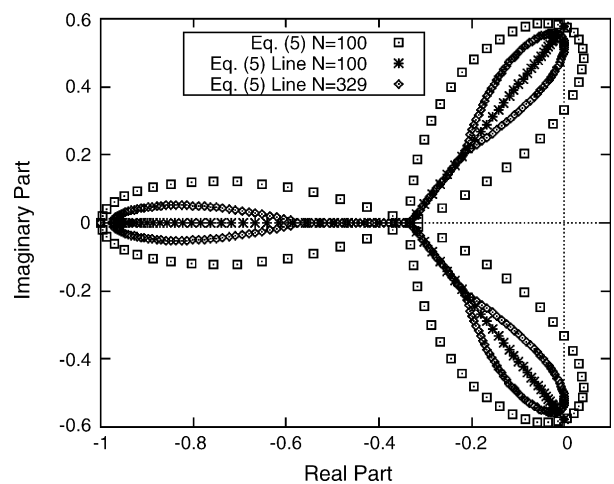


Fig. 10 – The eigenvalues for Eq. (5) exhibit a trefoil shape but those of the line system form a rotated Y at $s = 1$ and $N = 100$. As the number of species in the lines increases, the eigenvalues seem to approach those of the ring. This may be due to the fact that an infinitely long line is indistinguishable from a ring to those species far from the ends.

indistinguishable from a ring to the species far from the ends (Wildenberg et al., 2005).

The spatiotemporal patterns for the mirrored version of Eq. (2) appear very similar to those in Fig. 5, but do not connect at the top and bottom edges. It is probable that an increase in N will cause the dynamics of these line systems to behave similar to the ring system of equal dimension as the species far from the ends will see the same topology as those in a ring.

6. Conclusion

Adding spatial dependence to a Lotka–Volterra system through careful choice of the interaction matrix $A = (a_{ij})$ is relatively simple; however, the existence of a Lyapunov function prevents complex dynamics in certain regions of parameter space (reaction-diffusion Lotka–Volterra models also suffer from Lyapunov function limitations (Fitzgibbon et al., 1997)). All of the homogeneous spatial ring systems created with the above method have a circulant interaction matrix, and the regions where the Lyapunov function exists can be calculated. Knowledge of these regions can aid in numerical searches of the parameter space, drastically reducing the necessary computations. Despite this restriction of the parameter space these spatial systems can exhibit complex dynamics and produce interesting spatiotemporal patterns in their time series. It is notable that at high dimension the chaoticity (the value of the largest Lyapunov exponent) of the systems seems to lose its dependence on the dimension (Sprott et al., *in press*). This property may be useful when modeling systems where the number of competing species varies without drastic changes in the system's overall dynamics. It is also important to note that these systems appear to admit chaos regardless of their link reciprocity value, a measure of bidirectional vs. unidirectional connections within the system (Eq. (2) is perfectly reciprocal while Eq. (5) is slightly areciprocal) (Garlaschelli and Loffredo, 2004). This increases the versatility of these models as they may be used to represent the wide variety of topologies that are seen in real-world systems.

Line systems also provide a model for studying possible real-world systems. These systems admit chaos and periodicity, though the parameter space where these complex dynamics occur seems restricted compared to the ring systems. The eigenvalues of these line systems appear to approach those of the ring systems as the number of species in the line increases.

If it is necessary to allow the species' properties to change over time (a dynamic interaction matrix) then the method described above can be used with an adaptation algorithm (Sprott et al., 2005) yielding deterministic models that behave similar to the stochastic models of Neuhauser and Pacala (1999). This spatial dependence can also be extended to higher spatial dimensions (e.g. 2-D on the surface of a torus using a different organization of the interaction matrix) resulting in even more realistic models.

Uncited references

~~Boyce and DiPrima (2000); Gould and Eldridge (1977); and Marsden and McCracken (1976).~~

Acknowledgment

We are grateful to Mike Anderson, Jeff Noel, and Moe Hirsch for helpful discussion.

REFERENCES

- Brading, K., Castellani, E. (Eds.), 2003. *Symmetries in Physics: Philosophical Reflections*. Cambridge University Press, Cambridge, p. 458.
- Boyce, W.E., DiPrima, R.C., 2000. *Elementary Differential Equations and Boundry Value Problems*, seventh ed. John Wiley and Sons, New York, p. 768.
- Cantrell, R.S., Cosner, C., 2003. *Spatial Ecology via Reaction-Diffusion Equations*. John Wiley and Sons, England, p. 428.
- Coste, J., Peyraud, J., Couillet, P., 1979. Asymptotic behaviors in the dynamics of competing species. *SIAM J. Appl. Math.* 36, 516–543.
- Davis, P.J., 1994. *Circulant Matrices*, second ed. Chelsea, New York, p. 250.
- Fitzgibbon, W.B., Hollis, S.L., Morgan, J.J., 1997. Stability and Lyapunov functions for reaction-diffusion systems. *SIAM J. Math. Anal.* 28, 595–610.
- Frachbourg, L., Krapivsky, P.L., Ben-Naim, E., 1996. Spatial organization in cyclic Lotka–Volterra systems. *Phys. Rev. E* 54, 6186–6200.
- Freedman, H.I., 1987. *Deterministic Mathematical Models in Population Biology*, second ed. Marcel-Dekker, New York, p. 254.
- Garlaschelli, D., Loffredo, M.I., 2004. Patterns of link reciprocity in directed networks. *Phys. Rev. Lett.* 93, 268701.
- ~~Gould, S.J., Eldridge, N., 1977. Punctuated equilibrium: the temp and mode of evolution reconsidered. *Paleobiology* 3, 115–151.~~
- Hofbauer, J., Sigmund, K., 1988. *The Theory of Evolution and Dynamical Systems*. Cambridge University Press, Cambridge, U.K, p. 352.
- Kaplan, J., Yorke, J., 1979. Chaotic behavior in multidimensional difference equations. In: Peitgen, H.O., Walther, H.O. (Eds.), *Functional Differential Equations and Approximation of Fixed Points*, Lecture Notes in Mathematics, vol. 730. Springer, Berlin, pp. 228–237.
- LaSalle, J., Lefschetz, S., 1961. *Stability by Liapunov's Direct Method with Applications*. Mathematics in Science and Engineering, vol. 4. Academic Press, New York, pp. 134.
- Lotka, A.J., 1925. *Elements of Physical Biology*. Williams and Wilkins, Baltimore, p. 460.
- MacArthur, R., 1970. Species packing and competitive equilibrium for many species. *Theor. Pop. Bio.* 1, 1–11.
- Marsden, J.E., McCracken, M., 1976. *The Hopf Bifurcation And Its Applications*. Springer, New York, p. 408.
- May, R.M., 1973. *Stability and Complexity in Model Ecosystems*. Princeton University Press, Princeton, p. 235.
- Meinhardt, H., 1982. *Models of Biological Pattern Formation*. Academic Press, New York, p. 230.
- Murray, J.D., 1989. *Mathematical Biology*. Springer, Berlin, p. 718.
- Neuhauser, C., Pacala, S.W., 1999. An explicitly spatial version of the Lotka–Volterra model with interspecific competition. *Ann. Appl. Probab.* 9, 1226–1259.
- Ovaskainen, O., Hanski, I., 2003. Extinction thresholds in metapopulation models. *Ann. Zool. Fennici.* 40, 81–97.
- Provada, A., Tsekouras, G.A., 2003. Spontaneous formation of dynamical patterns with fractal fronts in the cyclic lattice Lotka–Volterra model. *Phys. Rev. E* 67, 056602.

- 420 Pykh, Y.A., 2001. Lyapunov functions for Lotka–Volterra
421 systems: an overview and problems. In: Proceedings of the
422 Fifth IFAC Symposium on Nonlinear Control Systems, pp.
423 1655–1660.
- 424 Sprott, J.C., 2003. *Chaos and Time-Series Analysis*. Oxford
425 University Press, New York, p. 507.
- 426 Sprott, J.C., 2004. Competition with evolution in ecology and
427 finance. *Phys. Lett. A* 325, 329–333.
- 428 Sprott, J.C., Vano, J.A., Wildenberg, J.C., Anderson, M.B., Noel,
429 J.K., 2005. Coexistence and chaos in complex ecologies.
430 *Phys. Lett. A* 335, 207–212.
- 431 Sprott, J.C., Wildenberg, J.C., Azizi, Y., *in press*. A simple
432 spatiotemporal chaotic Lotka–Volterra model. *Chaos*,
433 *Solitons, and Fractals*.
- 434 Takeuchi, Y., 1996. *Global Dynamical Properties of Lotka–*
435 *Volterra Systems*. World Scientific, Singapore, p. 302.
- 436 Turing, A.M., 1952. The chemical basis of morphogenesis.
437 *Philos. Trans. R. Soc. Lond. B* 237, 37–72.
- van den Driessche, P., Zeeman, M.L., 1998. Three-dimensional
438 competitive Lotka–Volterra systems with no periodic orbits.
439 *SIAM J. Appl. Math.* 58, 227–234.
- Volterra, V., 1926. Variazioni e fluttuazioni del numero
440 d’individui in specie animali conviventi, *Mem. R. Accad.*
441 *Naz. dei Lincei. Ser. VI* 2.
- Wildenberg, J.C., Vano, J.A., Sprott, J.C. 2005. Eigenvalue
442 animations for Lotka–Volterra ring systems. Available from
443 <http://sprott.physics.wisc.edu/chaos/eigeny.htm>.
444
- Wilson, W.G., De Roos, A.M., McCauley, E., 1993. Spatial
445 instabilities within the diffusive Lotka–Volterra system:
446 individual-based simulation results. *Theo. Pop. Biol.* 43, 91–
447 127.
- Li, X.-Z., Tang, C.-L., Ji, X.-H., 1999. The criteria for globally
448 stable equilibrium in n -dimensional Lotka–Volterra
449 systems. *J. Math. Anal. Appl.* 240, 600–606.
- Zeeman, M.L., 1997. *Circulant Lotka–Volterra Systems*,
450 unpublished manuscript.
451
452
453
454
455
456

UNCORRECTED PROOF